

# Electrical resistivity studies of $\text{Dy}(\text{Fe}_{1-x}\text{Co}_x)_2$ compounds

P. Stoch<sup>a</sup>, J. Pszczoła<sup>a,\*</sup>, P. Guzdek<sup>a</sup>, J. Chmista<sup>a</sup>, A. Pańta<sup>b</sup>

<sup>a</sup> Solid State Physics Department, AGH, Al. Mickiewicza 30, 30-059 Kraków, Poland

<sup>b</sup> Department of Metallurgy and Materials Engineering, AGH, Al. Mickiewicza 30, 30-059 Kraków, Poland

Received 19 October 2004; received in revised form 5 November 2004; accepted 8 November 2004

Available online 15 December 2004

## Abstract

Electrical resistivities of the  $\text{Dy}(\text{Fe}_{1-x}\text{Co}_x)_2$  intermetallic series were measured in a wide temperature region and the residual, phonon and magnetic contributions to the resistivities across the series were determined. The magnetic ordering temperatures were estimated for the  $\text{Dy}(\text{Fe}_{1-x}\text{Co}_x)_2$  compounds using the magnetic contribution to the electrical resistivity. The splitting energies between the 3d subbands of iron for the  $\text{Dy}(\text{Fe}_{1-x}\text{Co}_x)_2$  series were estimated using the magnetic hyperfine fields at  $^{57}\text{Fe}$  nuclei. The Curie temperatures obtained for the  $\text{Dy}(\text{Fe}_{1-x}\text{Co}_x)_2$  intermetallics and the Curie temperatures reported in the literature for the  $\text{Dy}(\text{Mn}_{1-x}\text{Fe}_x)_2$  and  $\text{Dy}(\text{Mn}_{0.4-x}\text{Al}_x\text{Fe}_{0.6})_2$  series correlate linearly with the squared energy splitting between the 3d subbands.

© 2004 Elsevier B.V. All rights reserved.

**Keywords:** Intermetallics; Crystal structure; Electrical resistivity; Curie temperatures; 3d subband splitting energy

## 1. Introduction

The heavy rare earth–transition metal ( $\text{RM}_2$ ) ferrimagnets are widely studied for a fundamental interest and for their practical applications [1–3]. Ferrimagnetism of the R–M compounds is a result of the coexistence between the 4f and 3d magnetism [4]. The electronic band structure of these intermetallics, and in particular that of their transition metal sublattice, is rather complex and poorly understood up to date.

It was previously found from the  $^{57}\text{Fe}$  Mössbauer effect studies of the  $\text{Dy}(\text{Mn}_{1-x}\text{Fe}_x)_2$  and  $\text{Dy}(\text{Fe}_{1-x}\text{Co}_x)_2$  pseudobinary series [5,6] that the  $^{57}\text{Fe}$  magnetic hyperfine field  $\mu_0 H_{\text{hf}}$  ( $\mu_0$  is the magnetic permeability) treated as a function of the average number  $n$  of 3d electrons calculated per transition metal site, resembles the Slater–Pauling plot, like in the case of the 3d metal–3d metal alloys [7,8]. This Slater–Pauling dependence mainly reflects the magnetism of the transition metal sublattice. At first, the strong ferromagnetism-type behaviour of the M-sublattice is observed. The magnetic hyperfine field

in the  $\text{Dy}(\text{Mn}_{1-x}\text{Fe}_x)_2$  series grows up with  $x$ . This growth is continued for the  $\text{Dy}(\text{Fe}_{1-x}\text{Co}_x)_2$  series, and the maximum value of the field is approached for the  $\text{Dy}(\text{Fe}_{0.7}\text{Co}_{0.3})_2$  compound (at  $x = 0.3$ ,  $n = 6.3$ ). At this Co-content the filling up of the majority 3d-subband by 3d-electrons is terminated. For the higher Co-substitutions the weak ferromagnetism-type behaviour of the M-sublattice appears. The filling-up of the minority 3d subband still proceeds and the observed field decreases gradually with  $n$  [5,6,9]. This Mn/Fe or Fe/Co replacement strongly influences the 3d-band and thus the magnetism and the hyperfine interactions of the compounds [5,6].

As the Mn/Fe or Fe/Co substitution changes the number  $n$  of 3d electrons in the M sublattice across the mentioned series it was interesting to study the influence of the 3d band population on the 4f(5d)–3d magnetism, on the magnetism of the 3d-sublattice and especially on the magnetic ordering temperatures  $T_C$ .

For this purpose the magnetic ordering temperatures  $T_C(x)$  for the  $\text{Dy}(\text{Fe}_{1-x}\text{Co}_x)_2$  series were determined from electrical resistivity measurements. Additionally, the literature  $T_C$  data for the  $\text{Dy}(\text{Mn}_{1-x}\text{Fe}_x)_2$  and  $\text{Dy}(\text{Mn}_{0.4-x}\text{Al}_x\text{Fe}_{0.6})_2$  series were taken into account [9,10]. These magnetic ordering

\* Corresponding author.

E-mail address: pszczoła@uci.agh.edu.pl (J. Pszczoła).

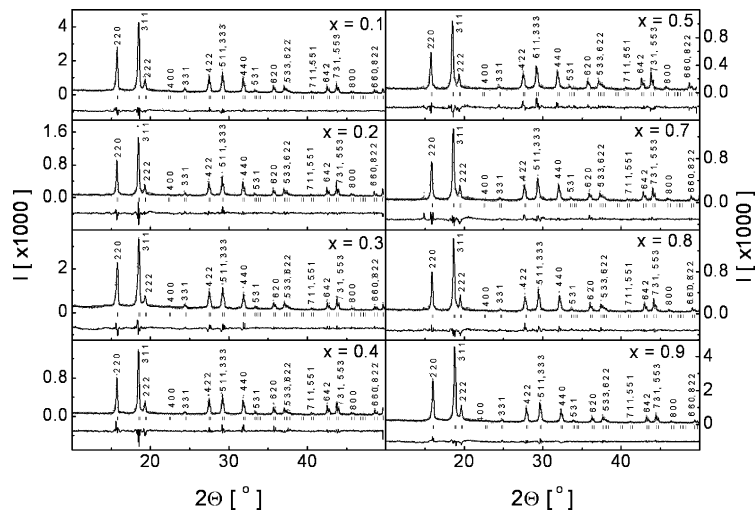


Fig. 1. X-ray powder diffraction patterns observed for the  $\text{Dy}(\text{Fe}_{1-x}\text{Co}_x)_2$  intermetallics (300 K). Fitted differential pattern is added below each diffractogram.  $I$  is the intensity and the capital letter  $\theta$  is the reflection angle.

temperatures are discussed qualitatively within the frame of the rigid band model.

## 2. The crystal structures

All  $\text{Dy}(\text{Fe}_{1-x}\text{Co}_x)_2$  ( $0 < x < 1$ ) compounds were prepared as cast by arc melting in a high purity argon atmosphere from the appropriate amounts of the Dy (99.9% purity), Fe, Co and Al (all 99.99% purity) starting materials.

The X-ray powder diffraction patterns were obtained for all the compounds using Mo  $K\alpha$  radiation at room temperature (patterns are presented in Fig. 1). For the all compounds the clean patterns corresponding to the cubic,  $\text{Fd}\bar{3}\text{m}$ ,  $\text{MgCu}_2$ -type (C15) Laves phase [11,12] were observed. The Rietveld-type procedure to fit the X-ray patterns was applied [13,14]. The crystal unit cell parameters  $a$  determined from the numerical analysis are presented in Fig. 2 and contained in Table 1. A considerable and nonlinear reduction of the  $a(x)$  parameter against the Co content  $x$  is observed. This dependence is well approximated by the numerical

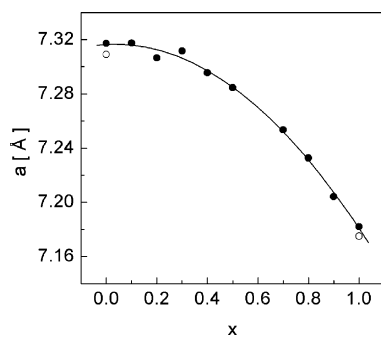


Fig. 2. The crystal lattice edge  $a$  of the  $\text{Dy}(\text{Fe}_{1-x}\text{Co}_x)_2$  intermetallics (300 K) for the  $\text{MgCu}_2$ -type structure (black points). Added exemplary literature data for  $\text{DyFe}_2$  and  $\text{DyCo}_2$  [1] (open points).

formula  $a(x) = [-0.145(13)x^2 + 0.010(13)x + 7.316(3)] \text{ \AA}$ . It is expected inspecting the experimental  $a(x)$  dependence (Fig. 2) that the physical errors  $\Delta a$  in some cases can be approximately even five times larger as compared to the numerical errors listed in Table 1. It is worth to notice that the literature parameters a known for  $\text{DyFe}_2$  and  $\text{DyCo}_2$ , the borderline compounds of the series [2,15,16] fit well to the obtained data (Fig. 2, Table 1).

## 3. Electrical resistivity (ER) studies

### 3.1. Resistivities

After arc melting a small part of the synthesized ingot was used each time to verify the crystal structure of the compound by the X-ray powder diffraction method. Bar (cuboid) shaped specimens with typical dimensions  $1 \text{ mm} \times 1 \text{ mm} \times 15 \text{ mm}$  used for electrical measurements were precisely cut from the ingots. Electrical contacts were established by point spark-welding of high purity thin copper wires onto the ends of the bars. After the welding procedure there was no microscopically observable cracks. The four probe method mentioned previously, was used to measure electrical resistivities [9].

The good quality electrical resistivities  $\rho$  as functions of temperature  $T$  obtained for the  $\text{Dy}(\text{Fe}_{1-x}\text{Co}_x)_2$  intermetallics are presented in Fig. 3. The electrical resistivity  $\rho(T; x)$  is expressed by the Matthiessen formula [17,18]:

$$\rho = \rho_0 + \rho_f + \rho_m \quad (1)$$

with the residual resistivity  $\rho_0$ , the phonon scattering resistivity  $\rho_f(T)$  and  $\rho_m(T)$  the magnetic contribution to resistivity (Fig. 3) [17–19]. The procedure to determine  $\rho_0$ ,  $\rho_f(T)$  and  $\rho_m(T)$  was somewhat improved as compared to the method described previously elsewhere [9].

Table 1

Crystal lattice parameter  $a$ , temperature  $\theta$ , residual resistivity  $\rho_0$ , magnetic hyperfine field  $\mu_0 H_{\text{hf}}$  [5,6], average number  $n$  of 3d electrons, squared splitting energy  $\Delta E^2$  and Curie temperature  $T_C$  of the  $\text{Dy}(\text{Fe}_{1-x}\text{Co}_x)_2$  intermetallics

$x$	$a$ [Å]	$\theta$ [K]	$D$ [ $\times 10^{-6} \Omega\text{m}$ ]	$\rho_0$ [ $\times 10^{-6} \Omega\text{m}$ ]	$\mu_0 H_{\text{hf}}$ [T]	$n$	$\Delta E^2$ [(eV) $^2$ ]	$T_C$ [K]
0	7.317(1) 7.309 [1] 7.325 [15]	256	0.0241	0.066(1)	22.68(28)	6.0	4.00	656(14) 635 [1] 635 [15]
0.1	7.317(1)	254	0.0197	0.249(1)	24.57(14)	6.1	4.37	693(13)
0.2	7.306(1)	281	0.0492	0.335(1)	25.53(25)	6.2	4.88	709(3)
0.3	7.312(1)	256	0.0816	0.311(1)	24.93(31)	6.3	4.84	707(8)
0.4	7.296(1)	260	0.0419	0.295(1)	25.53(52)	6.4	5.29	697(10)
0.5	7.285(1)	254	0.0437	0.294(2)	24.52(54)	6.5	4.54	673(6)
0.7	7.253(1)	243	0.0257	0.380(2)	–	6.7	–	552(1)
0.8	7.233(1)	211	0.0366	0.383(2)	21.45(85)	6.8	3.57	468(18)
0.9	7.204(1)	221	0.0408	0.266(2)	–	6.9	–	305(13)
1	7.182(1) 7.175 [1] 7.189 [16,20]	197	0.0297	0.176(2)	–	7.0	–	156(3) 123–169 [2] 140 [16]

To describe the procedure it is useful to mention that for the low temperature region ( $T \ll \theta$  and  $T \ll T_C$ ), the expression (1) can be written as [17,19]:

$$\rho(T) = 497.6D \left( \frac{T}{\theta} \right)^5 + AT^2 + BT + \rho_0 \quad (2)$$

with  $A$ ,  $B$ ,  $D$  and  $\theta$  being constants.  $\theta$  is a value close to the Debye temperature.

For the high temperature region ( $T \gg \theta$  and  $T \gg T_C$ ) the total resistivity can be approximated by the formula

[17,19]:

$$\rho(T) = D \left( \frac{T}{\theta} \right) + C \quad (3)$$

After fitting formula (2) to the experimental data  $\rho(T)$  for low temperatures and formula (3) to the experimental data for high temperatures the parameters  $D$ ,  $\theta$ ,  $A$ ,  $B$  and  $\rho_0$  present in the above equations were obtained. As a next step, the determined parameters were used as starting parameters to fit the low temperature  $\rho(T)$  data again to the full formula:

$$\rho(T) = D \left( \frac{T}{\theta} \right)^5 \int_0^{\theta/T} \frac{z^5}{(e^z - 1)(1 - e^{-z})} dz + AT^2 + BT + \rho_0 \quad (4)$$

valid for the electrical resistivity in the low temperature region [17–19].

The renewed parameters obtained from the last fitting, were used to calculate the phonon contribution  $\rho_f(T)$  using the integral part in formula (4) [9,17–19]. Subsequently subtracting from the experimental  $\rho(T)$  curve the corresponding fitted  $\rho_0$  value and the corresponding calculated temperature dependence of  $\rho_f(T)$ , the magnetic contribution versus temperature i.e. the  $\rho_m(T)$  curve was obtained for the particular compounds. The essential fitted parameters are presented in Fig. 4 and in Table 1. The less essential parameters  $A$ ,  $B$  and  $C$  are not presented in the table.

For instance, the remaining parameters, for the compound  $\text{Dy}(\text{Fe}_{0.6}\text{Co}_{0.4})_2$  were equal  $A = 1.3 \times 10^{-11} \Omega\text{m}/\text{K}^2$ ,  $B = -5.2 \times 10^{-10} \Omega\text{m}/\text{K}$ ,  $C = 1.33 \times 10^{-6} \Omega\text{m}$ . Similar values of the fitted parameters were obtained for the other compounds of the  $\text{Dy}(\text{Fe}_{1-x}\text{Co}_x)_2$  series. In fact, the less essential  $A$  and  $B$  parameters only improve somewhat the  $T^5$  dependence in formula (2) during the fitting procedure. The fitted values of temperatures  $\theta$  seem to be reasonable as compared to the Debye temperatures 420 K (for Fe), 385 K (for Co) and 140 K (for Dy) [17]. The Fe/Co substitution introduces a decreasing tendency in the temperature  $\theta$ , namely

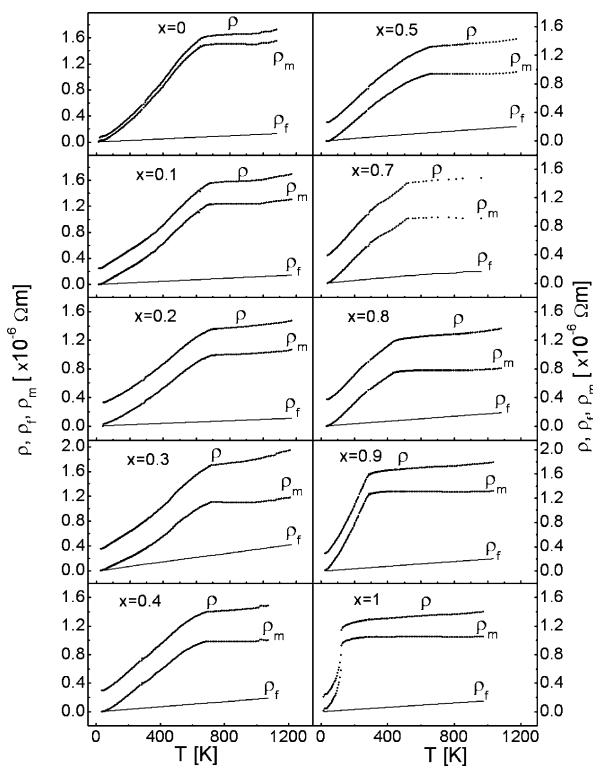


Fig. 3. Electric resistivities: the total  $\rho$ , the phonon  $\rho_f$  and the magnetic  $\rho_m$  observed against temperature for the intermetallics  $\text{Dy}(\text{Fe}_{1-x}\text{Co}_x)_2$ .

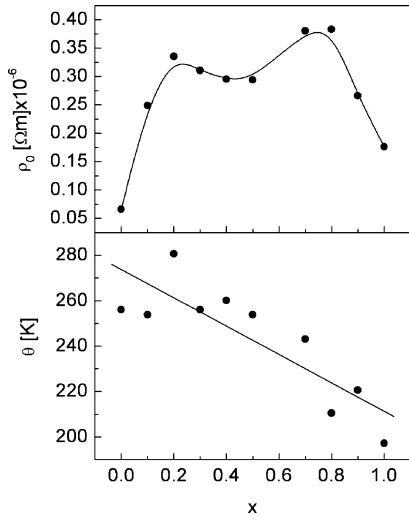


Fig. 4. The  $\rho_0$  and  $\theta$  parameters determined for the  $\text{Dy}(\text{Fe}_{1-x}\text{Co}_x)_2$  compounds.

$\theta(x) = [-62(4)x + 273(8)] \text{ K}$  (Fig. 4). The considerable distribution of the  $\theta$  values corresponding to the particular compounds in relation to the  $\theta(x)$  line can be ascribed to both the experimental (or numerical) errors and presumably to the individual properties of the compounds.

The residual resistivity  $\rho_0$  depends on both the crystal lattice imperfections and the statistical imperfections introduced by the random Fe/Co substitution. It is expected that the statistical disorder prevails. It seems that as a result of the statistical disorder the  $\rho_0$  parameter, a small value for  $x=0$ , increases with  $x$ , approaches a local maximum for  $x=0.25$ , decreases to a shallow local minimum at  $x=0.5$ , afterwards approaches a next local maximum at  $x=0.7$  and then decreases (Fig. 4).

### 3.2. Curie temperatures

It has been already discussed that the dependence  $\rho_m(T)$  is useful to determine the magnetic ordering temperatures  $T_C$  of the intermetallics [9]. The numerically determined  $\Delta\rho_m/\Delta T$  functions of temperature for the compounds of the  $\text{Dy}(\text{Fe}_{1-x}\text{Co}_x)_2$  series are presented in Fig. 5. The intersection of the two fitted straight lines gives the Curie temperature. The experimental error  $\Delta T_C$  of the method is quite considerable and for the particular compounds can approach even 20 K. The determined  $T_C$  temperatures are contained in Table 1 and Fig. 6 (open squares). Some  $T_C$  literature data for the  $\text{Dy}(\text{Fe}_{1-x}\text{Co}_x)_2$  series are also added (open rhombs [15,16,20]). Moreover data (black triangles) obtained using Mössbauer effect (ME) for the  $\text{Dy}(\text{Mn}_{1-x}\text{Fe}_x)_2$  series are also presented [9]. The substitution Mn/Fe and Fe/Co in the above mentioned series changes the number  $n$  of 3d electrons and thus induces the dependence of the Curie temperature on the composition of the compound. The value of  $T_C$  equals 45 K for the  $\text{DyMn}_2$  compound ( $n=5$ ) [21] and strongly increases across the  $\text{Dy}(\text{Mn}_{1-x}\text{Fe}_x)_2$  series to the value 656 K

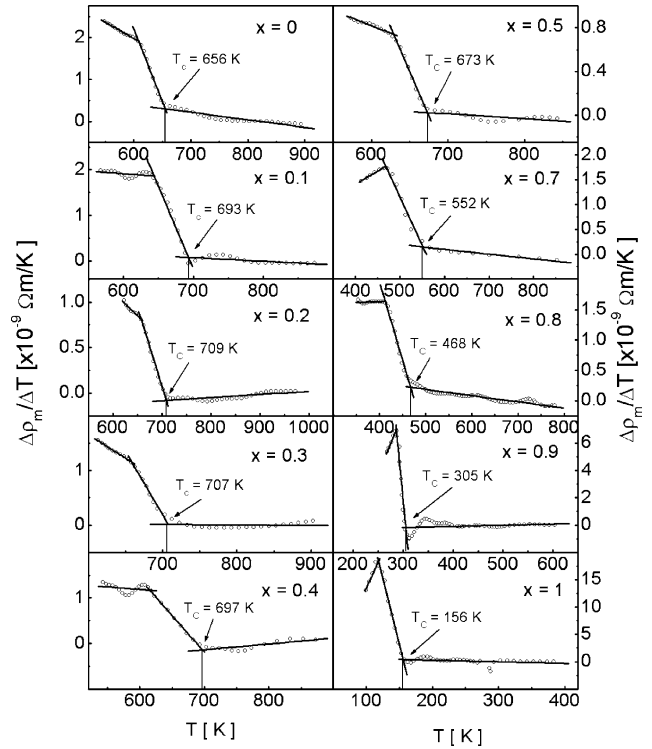


Fig. 5. The  $\Delta\rho_m/\Delta T$  functions of temperature for the  $\text{Dy}(\text{Fe}_{1-x}\text{Co}_x)_2$  compounds.

for the  $\text{DyFe}_2$  compound [2,15]. This growth is continued across the  $\text{Dy}(\text{Fe}_{1-x}\text{Co}_x)_2$  series and a maximal value  $T_C$  is approached in the area of the  $\text{Dy}(\text{Fe}_{0.7}\text{Co}_{0.3})_2$  compound ( $n=6.3$ ). Further the Fe/Co substitution strongly reduces the Curie temperature to the value 156 K for the  $\text{DyCo}_2$  compound [2,16]. There is no doubt that the  $T_C(n)$  dependence (Fig. 6) originates from the changes in the 3d band appearing across both the series. An attempt can be made to relate the  $T_C$  dependence to the 3d band properties.

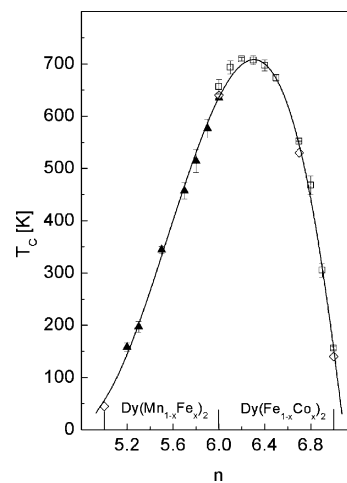


Fig. 6. The Curie temperatures  $T_C(n)$  or  $T_C(x)$  of the  $\text{Dy}(\text{Mn}_{1-x}\text{Fe}_x)_2$  (black triangles-ME) [9] and  $\text{Dy}(\text{Fe}_{1-x}\text{Co}_x)_2$  (open squares-ER; open rhombus [2,15,16]) intermetallics. Line follows experimental points.

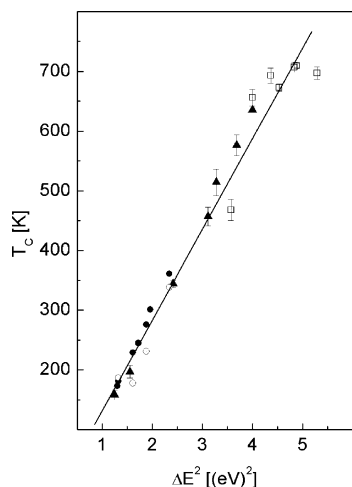


Fig. 7. The correlation between the Curie temperature  $T_C$  and the square value  $\Delta E^2$  of the splitting energy between the 3d subbands for the series Dy(Mn $_{1-x}$ Fe $_x$ ) $_2$  (black triangles-ME [9]), Dy(Mn $_{0.4-x}$ Al $_x$ Fe $_{0.6}$ ) $_2$  (black points-ME, open points-ER) [9] and Dy(Fe $_{1-x}$ Co $_x$ ) $_2$  (open squares-ER).

#### 4. Summary

It was discussed previously elsewhere that the ordering temperature  $T_C$  of the R–M intermetallics can be described by an empirical approximate formula  $T_C = T_R + T_M$  [1,3]. The  $T_R$  contribution originates from the rare earth sublattice and the  $T_M$  term arises from the transition metal sublattice. The contribution  $T_R = bG$ , where  $b$  is a certain constant and  $G$  the de Gennes factor [1,3]. It seems to be valid that the influence of the Mn/Fe and the Fe/Co substitution in the Dy(Mn $_{1-x}$ Fe $_x$ ) $_2$  and Dy(Fe $_{1-x}$ Co $_x$ ) $_2$  series on the  $T_R$  term is of the second order, if any. Thus the  $T_C$  dependence on  $n$  observed across the both series (Fig. 6) can be approximately ascribed to the  $T_M$  term. The  $T_M$  term however should be related to the 3d band changes in the M sublattice originated from the substitutions. Typically these substitutions should change the Fermi energy, the width of 3d bands, the position of the 3d bands in relation to the Fermi level, the 3d electron populations of the 3d subbands and the energy shift  $\Delta E$  between the 3d subbands [19,22,23]. To find these band properties is another not easy problem to study. Fortunately, some modest and useful results at this stage can be approached.

It was previously found for the DyFe $_2$  compound that the magnetic moment  $m_{3d}$  of the 3d electrons calculated per Fe atom equals to  $2 \mu_B$  [24]. As proposed elsewhere, assuming that the magnetic hyperfine field  $\mu_0 H_{hf}$  is approximately proportional to the  $m_{3d}$  moment a calibration constant  $K_1 = m_{3d}/\mu_0 H_{hf} = 2 \mu_B/22.68 \text{ T}$  can be introduced ( $\mu_0 H_{hf}$  for DyFe $_2$ —Table 1) [9].

This constant is used to calculate the  $m_{3d}(x)$  moments for the compounds of the considered substituted series from the known  $\mu_0 H_{hf}(x)$  data (Table 1) [9]. It was tested elsewhere for a number of 3d metals and alloys containing 3d metals that there is a linear correlation between the  $m_{3d}$  magnetic moment and the splitting energy  $\Delta E$  of 3d subbands [25,26].

It was found that this linear correlation is characterized by the ratio  $K_2 = \Delta E/m_{3d} = eV/\mu_B$  [25,26]. After using the ratios  $K_1$ ,  $K_2$  and the  $\mu_0 H_{hf}$  values, the splitting energies  $\Delta E$  between the 3d subbands at iron atoms were obtained across the studied series and the literature series [9]. Assuming additionally that the average  $\Delta E_{av}$  splitting between the 3d subbands in the M sublattice is proportional to the  $\Delta E$  splitting ( $\Delta E_{av} = K_3 \Delta E$ ;  $K_3$  is a constant) the magnetic ordering temperatures  $T_C$  can be related to the splitting energies  $\Delta E$ . Consequently a linear correlation between the magnetic ordering temperature  $T_C$  and the squared energy  $\Delta E^2$  is observed for the considered series of the RM $_2$  type intermetallics, as presented in Fig. 7. (This figure also contains data of the series Dy(Mn $_{0.4-x}$ Al $_x$ Fe $_{0.6}$ ) $_2$  [9].) The line in Fig. 7 is described by the numerical formula  $T_C(\Delta E^2) = [152(5)\Delta E^2 - 20(16)] \text{ K}$ . In this simple approach the only energy  $\Delta E$  was considered. This simplicity presumably can explain some deviations of the experimental points from the linear dependence.

The discussed series of compounds are relatively new and thus the other parameters related to the 3d band structure are unknown. Therefore at present a more subtle description is rather impossible. In fact, for certain rare earth–transition metal compounds the band structures were previously discussed and proposed, for instance in Refs. [27–29]. However, studies of the band structure of transition metal/transition metal substituted series and of transition metal/aluminium substituted series, similar to those series considered in the present paper, have not yet been carried out. Thus for a more developed description, a better knowledge of the band structure of the substituted intermetallic series would be useful. Therefore further experimental, theoretical and numerical studies would be helpful.

#### Acknowledgements

Supported partially by Polish Committee of Scientific Research, grant no. 4T08D03322. M. Mróz and T. Winek are acknowledged for technical assistance.

#### References

- [1] K.N.R. Taylor, Adv. Phys. 20 (1971) 551.
- [2] K.H.J. Buschow, in: E.P. Wohlfarth (Ed.), Ferromagnetic Materials, vol. 1, North-Holland, Amsterdam, 1980.
- [3] E. Burzo, H.R. Kirchmayr, in: K.A. Gschneidner Jr., L. Eyring (Eds.), Handbook on the Physics and Chemistry of Rare Earths, vol. 12, North-Holland, Amsterdam, 1989.
- [4] I.A. Campbell, J. Phys. F: Met. Phys. 2 (1972) L47.
- [5] B. Gicala, J. Pszczoła, Z. Kucharski, J. Suwalski, Phys. Lett. A 185 (1984) 491.
- [6] B. Gicala, J. Pszczoła, Z. Kucharski, J. Suwalski, Solid State Commun. 96 (1995) 511.
- [7] C.E. Johnson, M.S. Ridout, T.E. Cranshaw, Phys. Rev. Lett. 6 (1961) 450.
- [8] C.E. Johnson, M.S. Ridout, T.E. Cranshaw, Proc. Phys. Soc. 81 (1963) 1079.

- [9] P. Stoch, J. Pszczoła, P. Guzdek, J. Chmist, W. Bodnar, A. Jabłońska, J. Suwalski, A. Pańta, J. Alloys Compd., in press.
- [10] J. Pszczoła, J. Suwalski, Mol. Phys. Rep. 30 (2000) 113.
- [11] F. Laves, Naturwissenschaften 27 (1939) 65.
- [12] J. Chojnacki, Structural Metallography, Śląsk Press, Katowice, 1966.
- [13] H.M. Rietveld, J. Appl. Cryst. 2 (1969) 65.
- [14] J. Rodriguez-Carvajal, Physica B 192 (1993) 55.
- [15] A.S. van der Goot, K.H.J. Buschow, J. Less-Common Met. 21 (1970) 151.
- [16] F. Pourarian, W.E. Wallace, S.K. Malik, J. Less-Common Met. 83 (1982) 95.
- [17] F.J. Blatt, Physics of Electronic Conduction in Solids, McGraw-Hill, Michigan, 1968.
- [18] H. Ibach, H. Lüth, Solid State Physics, Springer, Berlin, 1995.
- [19] W. Vonsovskij, Magnetizm, Nauka, Moscow, 1971 (in Russian).
- [20] A. Ślebarski, J. Less-Common Met. 72 (1980) 231.
- [21] C. Ritter, S.H. Kilcoyne, R. Cywinski, J. Phys.: Condens. Matter 3 (1991) 727.
- [22] R.M. Bozorth, Ferromagnetism, Van Nostrand, Princeton, 1968.
- [23] J.M. Ziman, Principles of the Theory of Solids, Cambridge University Press, London, 1972.
- [24] O. Gunnarson, J. Phys. F: Met. Phys. 6 (1976) 587.
- [25] F.J. Himpsel, J.E. Ortega, G.J. Mankey, R.F. Willis, Adv. Phys. 47 (1998) 511.
- [26] F.J. Himpsel, J. Magn. Magn. Mater. 102 (1991) 55.
- [27] R. Coehoorn, J. Magn. Magn. Mater. 99 (1991) 55.
- [28] R. Coehoorn, K.H.J. Buschow, J. Magn. Magn. Mater. 118 (1993) 175.
- [29] R.F. Sabirianov, S.S. Jaswal, J. Appl. Phys. 79 (1996) 5942.